AKADÉMIAI KIADÓ

Tree growth optimization based control of grid-tied PV system

Mukul Chankaya[1*], Aijaz Ahmad[1] and Ikhlaq Hussain[2]

[1] Department of Electrical Engineering, National Institute of Technology Srinagar, Srinagar, India

[2] Department of Electrical Engineering, University of Kashmir, Srinagar, India

Pollack Periodica • An International Journal for Engineering and Information Sciences

17 (2022) 2, 8–13

DOI:
10.1556/606.2021.00470

Received: July 8, 2021 • Revised manuscript received: October 13, 2021 • Accepted: October 20, 2021
Published online: November 23, 2021

ORIGINAL RESEARCH PAPER

ABSTRACT

This paper presents a tree growth optimization based control of a grid-tied dual-stage photovoltaic system. The tree growth optimization has been employed for optimizing the proportional and integral controller gains for direct current bus voltage (V_{dc}) regulation to have minimum variation during dynamic conditions and to generate an accurate loss component of current (i_{Loss}). The accurate i_{Loss}, further enhance the control's performance by generating the accurate reference currents. The presented system is simulated and analyzed in a MATLAB simulation environment under various dynamic conditions, i.e., irradiation variation, unbalanced and abnormal grid voltage. The overall performance is satisfactory as per IEEE 519 standards.

KEYWORDS

photovoltaic, grid-tied, power electronics, power quality, optimization

1. INTRODUCTION

Worldwide, PhotoVoltaic (PV) installation is done at a humongous rate in both on-grid and off-grid configuration [1]. Various Meta-heuristic Optimization Techniques (MOTs) are implemented to improve the capability of grid-connected Renewable Energy Systems (RESs) [2, 3]. The Direct Current (DC) bus voltage (V_{dc}) is crucial for the stability of the system which is regulated by the conventional Proportional and Integral (PI) controller. For better stability, PI controller gains are optimized with the Jaya algorithm [4], and salp swarm optimization [5]. In [6], the comparison of Total Harmonics Distortion (THD) generated by Genetic Algorithm (GA) and Particle Swarm Optimization (PSO) is presented. In [7], Generalized Normal Distribution algorithm (GNDA), and in [8], Firefly Optimization Algorithm (FOA) along with GA are implemented to achieve better V_{dc} stability. In [9], comparison of V_{dc} stability and THD with Whale Optimization Algorithm (WOA), Ant Lion Optimization (ALO), Moth Flame Optimization (MFO) and Grey Wolf Optimization (GWO) is presented.

This paper presents the Tree Growth Optimization (TGO) technique [10] based Voltage Source Converter (VSC) control of a grid-tied dual-stage PV system. The presented system directly transfers the PV power to the grid in the absence of any local load. The main contributions of the presented work are:

1. TGO regulated DC link delivers more stable V_{dc} with reduced variations during diverse dynamic conditions, i.e., irradiation variation, abnormal and unbalanced grid voltage conditions;
2. TGO regulated DC link generates accurate i_{Loss} current, which further enhances the VSC performance and improves the quality of power delivered to the grid.

*Corresponding author.
E-mail: mukulchankaya@gmail.com

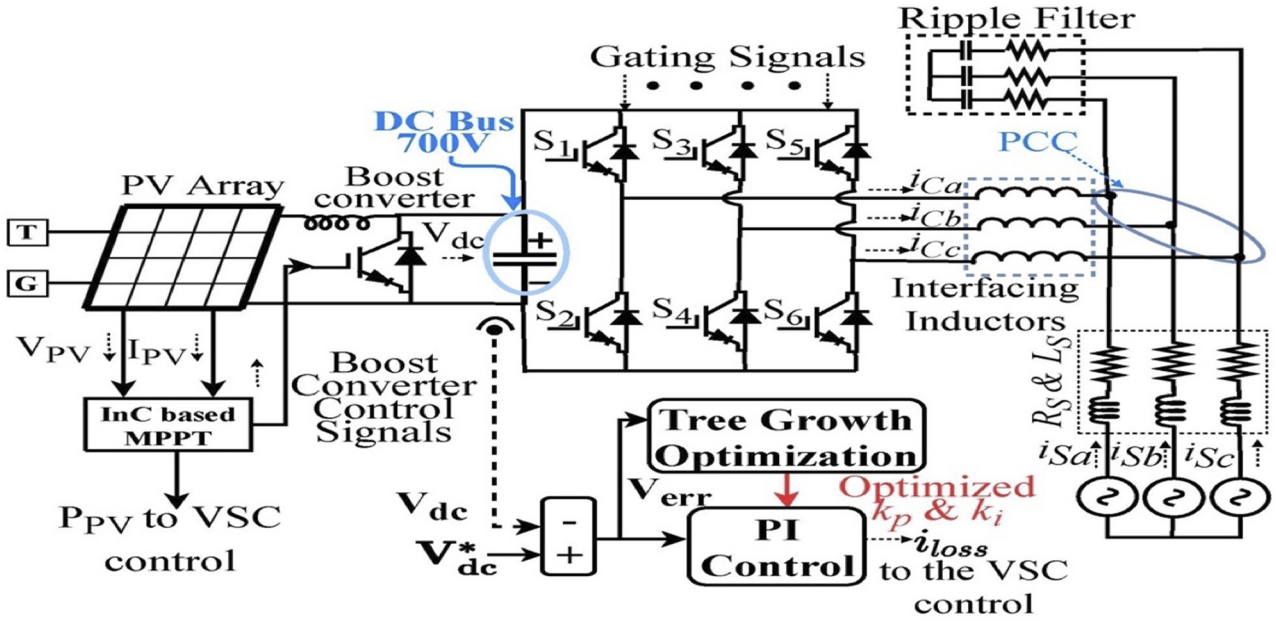

Fig. 1. Proposed topology

2. PROPOSED TOPOLOGY

Figure 1 shows a double-stage grid-connected PV system. PV array is configured using Kyocera 200 GT module, where 23 and 7 modules are connected in series and parallel to provide PV voltage (V_{PV}) of 605 V and PV current (I_{PV}) of 56 A. The boost converter, is controlled by the Incremental Conductance (InC) based Maximum Power Point Tracking (MPPT) algorithm. The three-phase VSC via interfacing inductor, ripple filter and Alternating Current (AC) grid of 415 V (r.m.s.) at 50 Hz are connected to the Point of Common Coupling (PCC). The interfacing inductor and ripple filter reduces the voltage and current ripples entering the grid.

3. TREE GROWTH OPTIMIZATION

Like any other MOT, TGO is also executed in two phases exploration and exploitation as it is shown in Fig. 2. The TGO separates the trees into four groups as N1, N2, N3 and N4 [10]. The N1 trees group involves the better trees, which will grow easily with accessible food and light. The N2 trees group includes somewhat good trees, which compete with the N1 group for sunlight by approaching the nearest best tree at different angles. The N3 trees groups belong to the worst trees, which shows very little growth due to the scarcity of food and sunlight and will be eliminated during the optimization process. The N4 trees group is the new population (1), which replaces the deleted N3 group. The population gets updated in every iterations (2), which reduces the local minima stagnation chances and balances the exploration and exploitation stage. TGO is initiated with a random population of $k = 50$ trees, decision variables as PI gains ($i = 2$) and the upper and lower bounds ($u_b = 5$, $l_b = 0$), maximum iterations as $j = 50$,

$$N4 = N1{*}N2 + N3, \tag{1}$$

$$\text{New pop} = \text{New pop} + N4. \tag{2}$$

The fitness function of trees is calculated (3) in the exploration phase, where T_i^{k+1} is the tree fitness function, θ

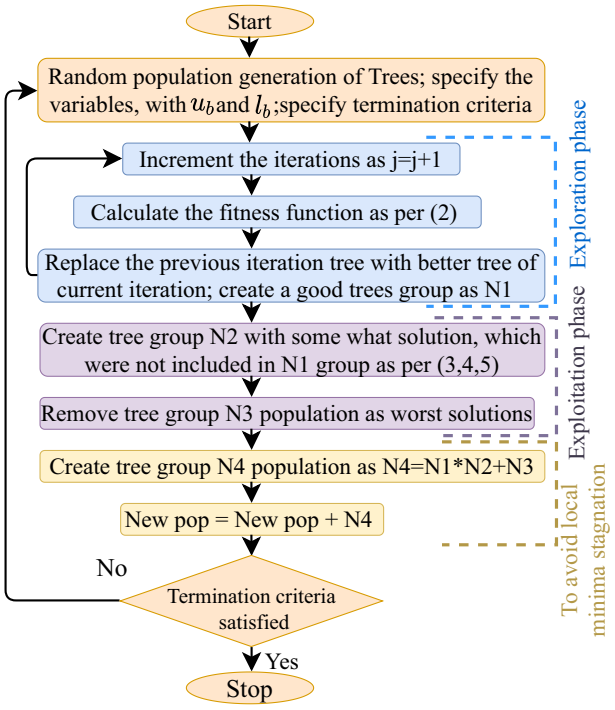

Fig. 2. Flow chart of tree growth optimization

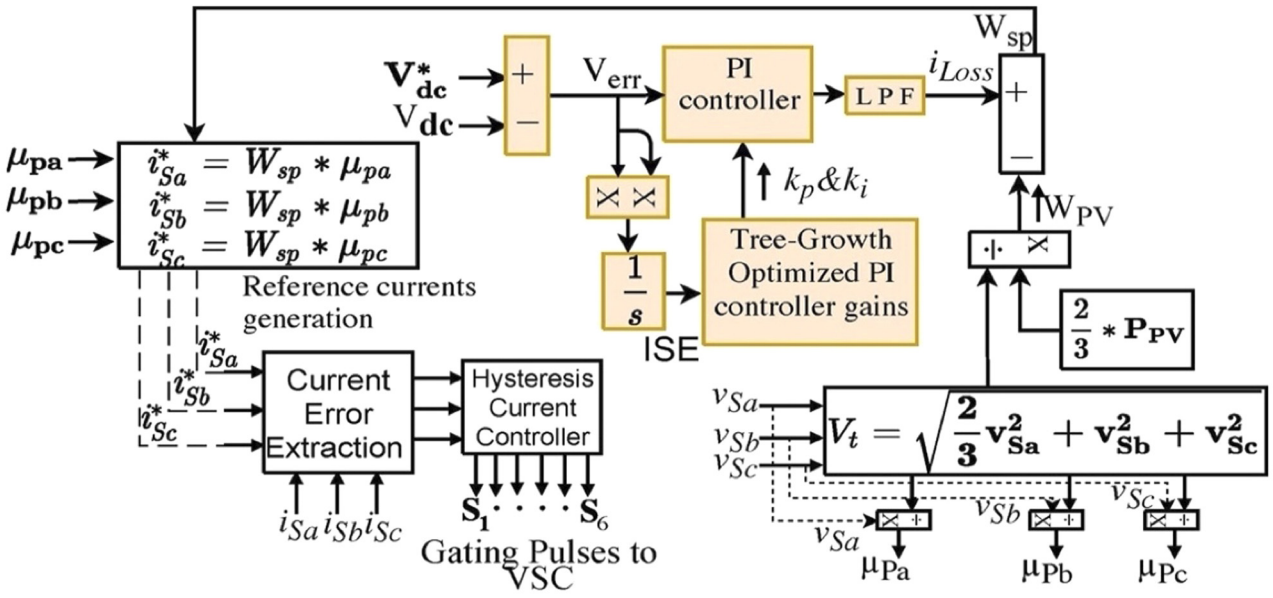

Fig. 3. VSC and V_{dc} control

is the tree reduction rate and r is the random variable between [0,1],

$$T_i^{k+1} = \frac{T_i^k}{\theta} + r \times T_i^k, \text{ for } k = 1, 2, 3 \ldots, 50, \text{ and } i = 1, 2. \tag{3}$$

The N2 tree group members have to move distance at various angles for sufficient food and sunlight, which is d_i calculated (4). The linear combination between trees is developed by selecting the two solutions as x_1 and x_2 with minimum distance d_i (5), where λ is the random variable between [0,1] and y is the location of the best tree, approached by N2 tree members,

$$d_i = \left(\sum_{i=1}^{N1+N2} \left(T_{N2}^k - T_i^k \right)^2 \right)^{1/2}, \quad d_i = \begin{cases} d_i & \text{if } T_{N2}^k \neq T_i^k, \\ \infty & \text{if } T_{N2}^k = T_i^k, \end{cases} \tag{4}$$

$$y = \lambda x_1 + (1 - \lambda) x_2. \tag{5}$$

The new position of N2 tree members will be updated (6), where α_i is the angle at which N2 members extends towards better food and sunlight. α_i is also a random variables between [0,1],

$$T_{N2}^k = T_{N2}^k + \alpha_i y. \tag{6}$$

The TGO delivers optimal gains of PI controller for DC bus regulation after hitting the termination criteria.

4. PROPOSED CONTROLS

The proposed system is made functional by utilizing three controls, i.e., InC based MPPT control, TGO based V_{dc} control and VSC control.

4.1. Tree-growth optimized V_{dc} control

Figure 3 shows TGO regulated V_{dc}, where V_{dc} is sensed at the DC bus and compared with the reference V_{dc} $\left(V_{dc}^{ref} = 700\,\text{V}\right)$ to generation of Integral Square Error (ISE) as an objective function (7) to be minimized by the TGO and deliver optimal gains [4],

$$ISE = \int_0^t \left(V_{dc}^{ref} - V_{dc} \right)^2 = \int_0^t V_{err}^2. \tag{7}$$

4.2. VSC control

Figure 3 shows VSC control, which is simulated without load, so the generated reference currents will be the function of unit templates and overall weight signal (W_{sp}) [7]. The unit templates $(\mu_{Px}$; where $x = a, b, c)$ are generated as a function of grid phase voltage $(v_{Sx};\ x = a, b, c)$ and voltage magnitude (V_t) (8).

The W_{PV} represents the PV power inserted in the grid is calculated (9), where PV current (I_{PV}), voltage (V_{PV}) and power (P_{PV}) are delivered by the PV array.

The W_{sp} is calculated as a function of W_{PV} and i_{Loss} (10). The optimized DC bus generates an accurate i_{Loss} which will produce better W_{sp} with reduced ripples, The reference current $(i^*_{Sx}$; where $x = a, b, c)$ for each phase are generated (11). The error current signals are generated by comparing i_{Sabc} and i^*_{Sabc} and delivered to the hysteresis current controller for the VSC switching signals generation.

$$\mu_{px} = \frac{v_{Sx}}{V_t} = \frac{v_{Sx}}{\sqrt{\frac{2}{3}\left(v_{Sa}^2 + v_{Sb}^2 + v_{Sc}^2\right)}}, \text{ where } x = a, b, c, \tag{8}$$

$$W_{PV} = \frac{2}{3}\frac{P_{PV}}{V_t} = \frac{2}{3}\frac{I_{PV} * V_{PV}}{V_t}, \tag{9}$$

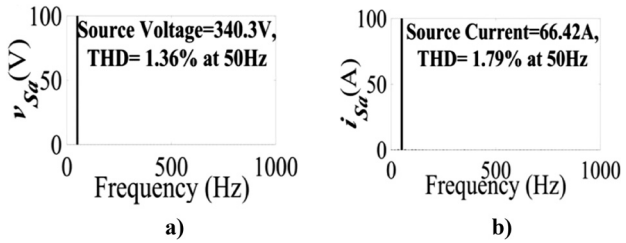

Fig. 4. THD levels of a) v_{Sa} and b) i_{Sa}

$$W_{sp} = i_{Loss} - W_{PV}, \tag{10}$$

$$i^*_{Sx} = \mu_{px} \cdot W_{sp}, \text{ where } x = a, b, c. \tag{11}$$

5. RESULTS AND DISCUSSIONS

The proposed system is analyzed under steady-state and various dynamic conditions in a MATLAB simulation environment.

5.1. Steady-state analysis

Figure 4 shows the THD levels of v_{Sabc} and i_{Sabc}, which are acceptable as per IEEE519 standard [11], and ensures better power quality of the system.

5.2. Irradiation variation analysis

During irradiation change, solar irradiation level is reduced from 1000 W m^{-2} to 600 W m^{-2} and restored to 1000 W m^{-2}. Figure 5 shows the v_{Sabc} and i_{Sabc} are inexact phase opposition as PV generated power is delivered to the grid (P_g). The i_{Sabc} follows i^*_{Sabc} generated by the VSC control. The phase a of compensator current (i_{Ca}) is out of phase with i_{Sabc} as P_g is being provided to the grid. The i_{Ca} magnitude changes with P_g

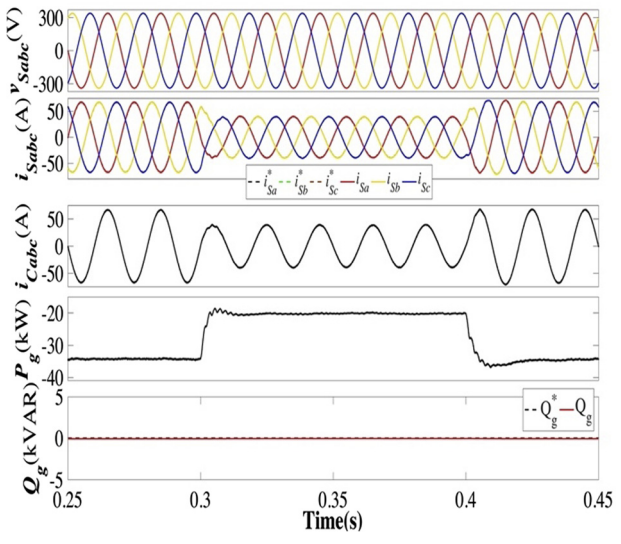

Fig. 5. Irradiation variation analysis of v_{Sabc}, i_{Sabc}, i_{Ca}, P_g and Q_g

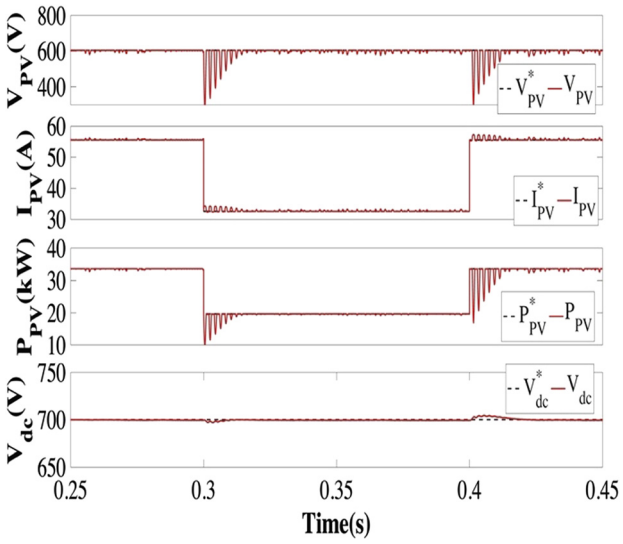

Fig. 6. Irradiation variation analysis of V_{PV}, I_{PV}, P_{PV} and V_{dc}

during irradiation change. The reactive power (Q_g) requirement of the system is zero, which follows its reference ($Q^*_g = 0$). On the DC side, the V_{PV} remains at the desired value of 605 V as V^*_{PV} with the help of a boost converter. The I_{PV} and P_{PV} changes with the irradiation change as per their reference values, i.e., I^*_{PV} and P^*_{PV}. The V_{dc} is maintained at the appropriate level of 700 V as it is shown in Fig. 6.

5.3. Abnormal grid voltage analysis

Figure 7 shows grid voltage sag and swell of 20% is simulated. The v_{Sabc} remains 180° out of phase w.r.t. i_{Sabc}. The i_{Sabc} magnitude increases with voltage sag and then reduces with voltage swell and vice versa applies to i_{Ca}. The P_g initially changes with the abnormal grid voltage but soon settles down to its desired value. The Q_g remains zero. Figure 8

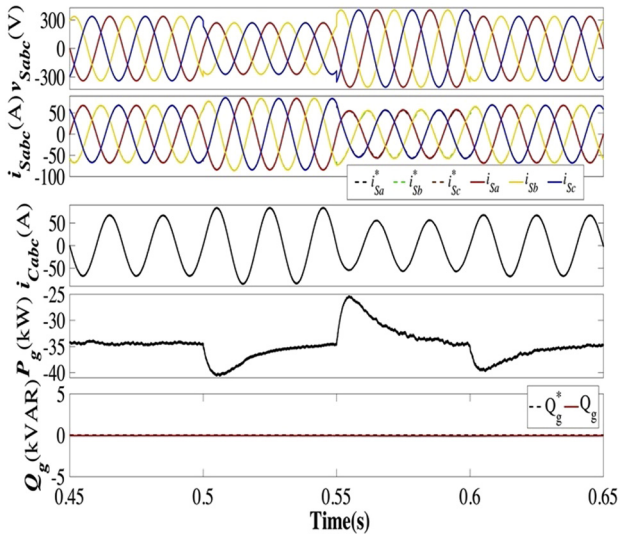

Fig. 7. Abnormal grid voltage analysis of v_{Sabc}, i_{Sabc}, i_{Ca}, P_g and Q_g

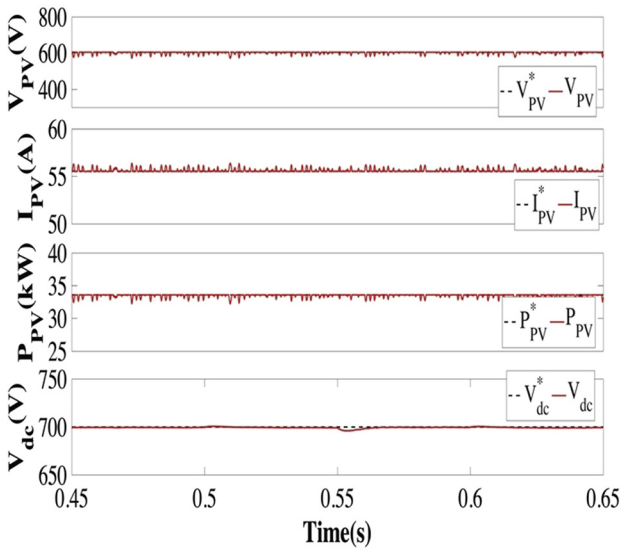

Fig. 8. Abnormal grid voltage analysis of V_{PV}, I_{PV}, P_{PV} and V_{dc}

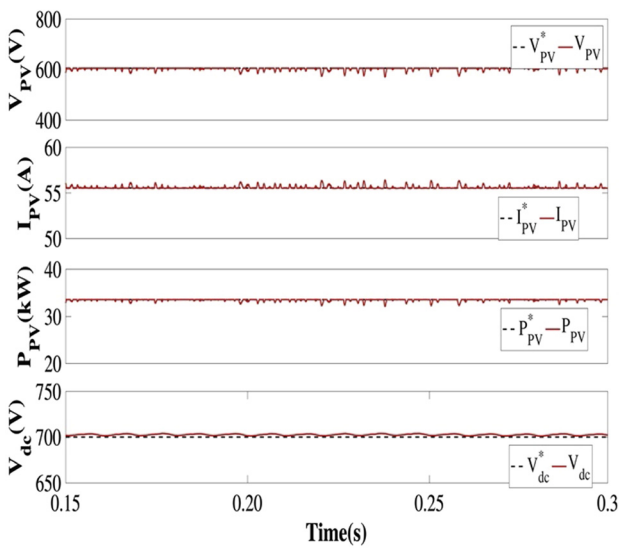

Fig. 10. Unbalanced grid voltage analysis of V_{PV}, I_{PV}, P_{PV} and V_{dc}

shows V_{PV}, I_{PV} and P_{PV} remains unchanged as their reference values, i.e., V^*_{PV}, I^*_{PV} and P^*_{PV}. The V_{dc} is kept at the required level of 700 V.

5.4. Unbalanced grid voltage analysis

During grid voltage unbalancing, magnitude of the phase *a* of the grid is reduced. The i_{Sabc} follows i^*_{Sabc}, with a small mismatch in phase *b* and *c* currents. The Q_g exchange with the grid is kept around zero as Q^*_g as it is shown in Fig. 9. On the DC side, V_{PV}, I_{PV} and P_{PV} follows V^*_{PV}, I^*_{PV} and P^*_{PV}. Figure 10 shows V_{dc} is kept at 700 V.

5.5. Tree-growth optimized DC bus analysis

The TGO based V_{dc} variations have significantly reduced during the induced dynamic condition in a simulation environment. The comparison of TGO, GA and manually

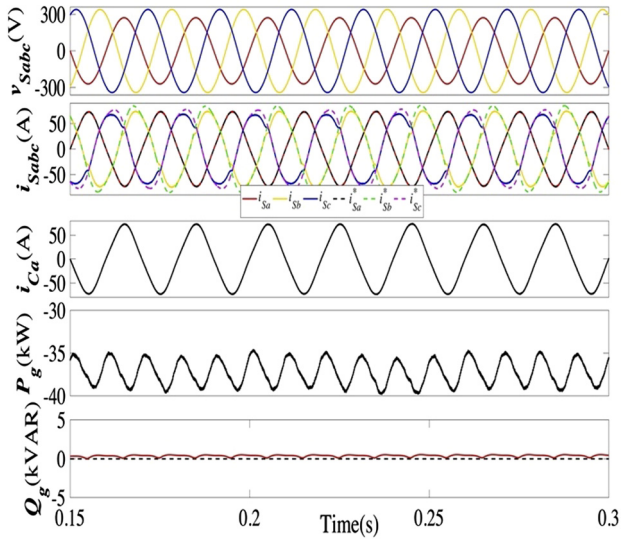

Fig. 9. Unbalanced grid voltage analysis of v_{Sabc}, i_{Sabc}, i_{Ca}, P_g and Q_g

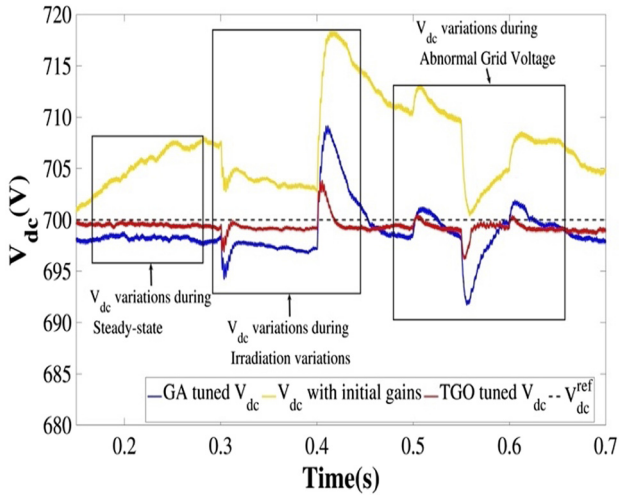

Fig. 11. Tree-growth optimized DC bus voltage analysis

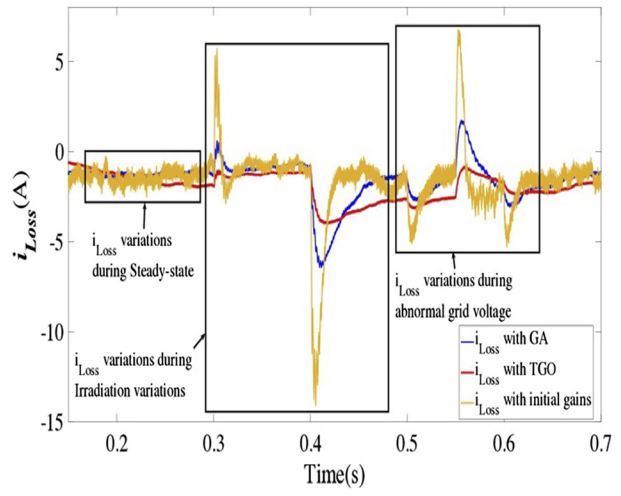

Fig. 12. Tree-growth optimized i_{Loss} current analysis

tuned V_{dc} is presented in Fig. 11. The optimized DC bus produces an accurate i_{Loss} current with reduced ripples which enhances the operational capability of the VSC control and results in the generation of accurate weight signals as it is shown in Fig. 12.

6. CONCLUSION

The performance of a grid-tied dual-stage PV system with tree growth optimized VSC control has been presented. The TGO delivers the optimal PI controller gains for DC bus regulation. The TGO regulated DC bus voltage have reduced variations during dynamic conditions in comparison with GA, as well as, generates an accurate loss component of current which further improves the VSC performance by generating precise reference currents. The presented system is observed under steady-state, and diverse dynamic conditions, i.e., irradiation variation, unbalanced and abnormal grid voltage, and found performing satisfactorily as per IEEE 519 standards.

ACKNOWLEDGMENTS

The work reported herewith has been supported by J&K Science Technology and Innovation Council, Department of Science and Technology, Jammu & Kashmir (JKST&IC/75/2020).

REFERENCES

[1] O. Gandhi, D. S. Kumar, C. D. Rodríguez-Gallegos, and D. Srinivasan, "Review of power system impacts at high PV penetration Part I: Factors limiting PV penetration," *Sol. Energy*, vol. 210, pp. 181–201, 2020.

[2] F. S. Sergio, Z. F. Desta, and P. S. C. Jao, *Optimization in Renewable Energy Systems, Recent Perspective*. Butterworth-Heinemann, 2017.

[3] I. E. Haber, G. Bencsik, B. Naili, and I. Szabo, "Building thermal capacity for peak shifting, based on PV surplus production," *Pollack Period.*, vol. 16, no. 2, pp. 117–123, 2021.

[4] S. Mishra and P. K. Ray, "Power quality improvement using photovoltaic fed DSTATCOM based on JAYA optimization," *IEEE Trans. Sustain. Energy*, vol. 7, no. 4, pp. 1672–1680, 2016.

[5] M. Chankaya, I. Hussain, A. Ahmad, I. Khan, and S. M. Muyeen, "Nyström minimum kernel risk-sensitive loss based seamless control of grid-tied PV-hybrid energy storage system," *Energies*, vol. 14, no. 5, pp. 1–24, 2021.

[6] T. P. Kalaignan, J. S. Kumar, and Y. Suresh, "PSO and GA based performance optimization of PI controller in three phase shunt hybrid filter," *Int. Jour. Engg. Res. Tech.*, vol. 3, no. 8, pp. 255–260, 2014.

[7] M. Chankaya, I. Hussain, A. Ahmad, H. Malik, and F. P. G. Márquez, "Generalized normal distribution algorithm-based control of 3-phase 4-wire grid-tied PV-hybrid energy storage system," *Energies*, vol. 14, no. 14, pp. 1–24, 2021.

[8] L. Kota and K. Jarmai, "Improving optimization using adaptive algorithms," *Pollack Period.*, vol. 16, no. 1, pp. 14–18, 2021.

[9] N. Aouchiche, "Meta-heuristic optimization algorithms based direct current and DC link voltage controllers for three-phase grid connected photovoltaic inverter," *Sol. Energy*, vol. 207, 2019, pp. 683–692, 2020.

[10] A. Cheraghalipour, M. Hajiaghaei-Keshteli, and M. M. Paydar, "Tree growth algorithm (TGA): A novel approach for solving optimization problems," *Eng. Appl. Artif. Intell.*, vol. 72, pp. 393–414, 2018.

[11] D. Committee, I. Power, and E. Society, "IEEE recommended practice and requirements for harmonic control in electric power systems," in *IEEE Std 519-2014 (Revision of IEEE Std 519-1992)*, pp. 1–29, 2014.